Laser driven fast electron collimation by magnetic fields from structured targets

Contact **bramakrishna01@qub.ac.uk**

B. Ramakrishna, S. Kar, D. J. Adams, K. Markey, M. Borghesi and M. Zepf
School of Mathematics and Physics, Queen's University of Belfast, Belfast, BT7 1NN, UK

M. Quinn, X. Yuan and P. Mckenna
SUPA, Department of Physics, University of Strathclyde, Glasgow G4 0NG, UK

A. Henig and D. Kiefer
Max-Planck Institut for Quantumoptik, Garching, Germany

A. P. L. Robinson, K. L. Lancaster, J. S. Green and P. A. Norreys
Central Laser Facility, STFC, Rutherford Appleton Laboratory, HSIC, Didcot, Oxon OX11 0QX, UK

J. Schreiber and C. Bellei
Blackett Laboratory, Imperial College London, Prince Consort Road, London SW7 2BZ, UK

Abstract
Collimation of relativistic electron beams is achieved experimentally by using structured targets. We compare the transport of hot electrons produced during the interaction of an ultra intense laser pulse through the structured target and flat targets. Results confirm that effective collimation of electron beams is realized by employing structured targets which have a radial discontinuity in the atomic number Z. The ability to control the electron flow allows substantial additional freedom in the design of fast ignitor targets as well as allowing increased coupling efficiency to the hot spot by suppressing angular spread.

Introduction
Generation of relativistic electron beams is a core aspect in intense laser ($I > 10^{18}$ W/cm^2) solid interactions. Electrons are accelerated by resonance absorption [1], Vacuum heating [2] and J×B heating [3] and subsequently penetrate into the target. The understanding of relativistic electron transport is a prerequisite for many applications of ultraintense lasers, notably fast ignition and proton acceleration from solid targets.

In the recent past, fast electron transport into solids has been experimentally investigated by means of optical [4], X-ray [5-7] and proton diagnostics [8-9]. These experiments have shown that the electrons propagate into the target with a divergence of typically 40-50°. Such large divergence has important implications for viable experimental geometries in the fast ignition scheme for inertial fusion [10]. The most important is that the source of fast electrons must be placed in the immediate vicinity of the compressed fuel, thereby placing tight constraints on the cone design of advanced Fast Ignitor Scheme [11]. A particular concern is the trade-off between a sufficient wall thickness to ensure the cone remains intact at bang-time and close proximity of the electron source to ensure efficient coupling.

A successful guiding and collimation scheme would relax these constraints substantially and also allow focusing of the electron beam. The latter capability allows the primary electron source size to be determined independently from the size of the hot-spot and hence makes the minimum ignition pulse ponderomotive potential a free parameter (which controls the electron energy). This is a very important development, since it may allow an optimised point design at 1μm laser wavelength resulting in substantially reduced ignition laser requirements.

Here we report the first evidence of successful collimation in two dimensions using structured targets with sharp radial boundaries in the target atomic number Z.

Theory
The experiment reported here is based on the theoretical work by Robinson and Sherlock [12] and our recent proof of principle experiment [13]. Robinson and Sherlock suggest that targets with a sharp radial boundary in resistivity should lead to the growth of collimating magnetic fields that confine the fast electrons to the high resistivity region. The growth of the collimating fields can be understood from combining Faraday's law with Ohm's law:

$$\frac{\partial B}{\partial t} = \eta \nabla \times j + (\nabla \eta) \times j.$$

Where η is the resistivity and j is the fast electron current density. The first term corresponds to magnetic fields that act to push fast electrons towards regions of higher fast electron density, while the second term pushes the fast electrons towards regions of higher resistivity. This implies that a target with a sharp radial resistivity boundary should build up strong magnetic fields at the boundary that can collimate the flow of fast electrons [12]. Here we used the Z dependence of the target resistivity to achieve this aim: The target is engineered in such a way that the central material ('wire') has a higher resistivity than the surrounding material ('cladding'). The material chosen for this experiment were 25 or 50 μm Fe wires surrounded by aluminium to make up a total target radius of 250 μm. Important factors in the choice of material configuration are to ensure that the high Z material also has higher cold resistivity to ensure that

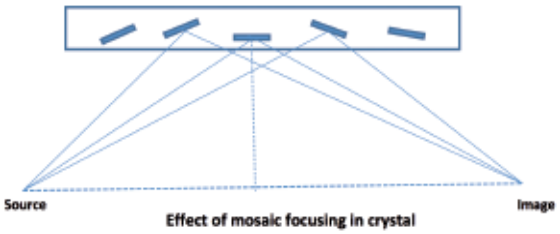

Figure 1. Mosaic parafocusing effect in HOPG crystal.

correct sign of the resistivity gradient across the full range of target temperatures as well as manufacturing issues. The results of the structured targets was compared to uniform thin foil targets (Cu, Fe, Al).

The primary diagnostic of the collimation was K-α radiation emitted from a 10 μm Cu tracer layer at the rear side of all the targets. The size of the emitting region was diagnosed using an X-ray pin-hole camera, spherical quartz crystal imager and via source broadening using a HOPG spectrometer.

The best quality data was obtained from the HOPG crystal and the pinhole camera. The imaging crystal did not provide enough signal for the targets with long wires where the collimation effect is the clearest. The mosaic structure of the HOPG crystal made it particularly effective for this experiment, because the unique crystal plane structure results in a combination of highly efficient X-ray diffraction, low spectral resolution and mosaic focusing[14]. This combination of characteristics means that for our experimental conditions the width of the K_α line is dominated by source broadening and hence provides a high brightness measure of the K_α source size. Briefly the mosaic structure (figure 1) allows several rays with same energy coming from a point source to be diffracted by different crystallites inside the mosaic crystal according to Bragg's law. This requires that the ray has to travel inside the crystal until it finds a crystallite with correct orientation resulting in the diffracted rays converging to single point. The crystal to source distance and the source to crystal distance are equal so that the parafocusing effect happens in a magnification of 1:1. The HOPG crystal used in the experiment is ZYA crystal with mosaic spread of 0.40. The reliability of extracting source size information from the source broadening of the spectral line was confirmed by comparing pinhole and HOPG data from the same shots. Figure 4 shows that the agreement is excellent and demonstrates that HOPG line broadening is indeed a good way to measure the X-ray source size and that source broadening dominates the measured line-shape.

The spectral line broadening is indeed negligible also becomes clear when observing the HOPG signal from thin Cu foils (figure 5). For such shots we observe not only the K_α and K_β lines but also the thermally excited He_α and Ly_α lines, demonstrating that a Cu plasma with temperatures above 1 keV was formed. For such hot plasmas Doppler line broadening becomes significant. However the measured line width for plasmas showing the thermally excited emission lines is much smaller than for thick targets with cold Cu emission regions (i.e. no He_α and Ly_α visible), confirming that the actual linewidth does not affect the measured linewidth for our parameters.

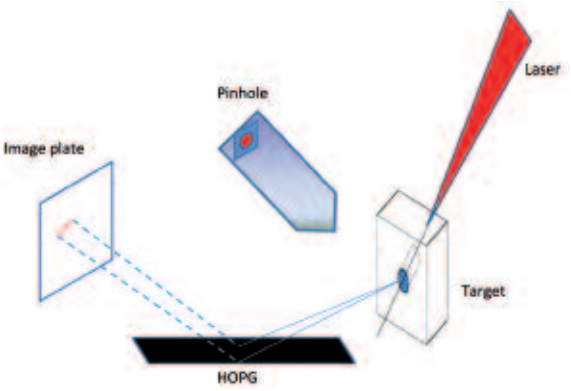

Figure 2. Experimental configuration inside the chamber.

The experiment was performed at Rutherford Appleton Laboratory employing Vulcan Petawatt laser system. After reflection from a plasma mirror[16], the laser pulse delivered 150 J of energy on target in FWHM duration of 1 ps. The laser was focused to a peak intensity of 10^{20} W/cm^2 on target at 5° angle of incidence. The experimental set up is depicted in fig 2.

We have measured the Cu K_α radiation from targets with a thickness ranging from 5-250 μm. The source to crystal distance and the crystal to detector distance was 165 mm respectively with the crystal set at a Bragg angle of 13.30. A range of diagnostics were employed in the campaign but we restrict the discussion in this paper to X-ray pin hole images and HOPG spectrum. The Cu K_α radiation (8.05 keV) emitted from the target was focused by the flat HOPG crystal on to an image plate as shown in fig 2.

Results and discussion

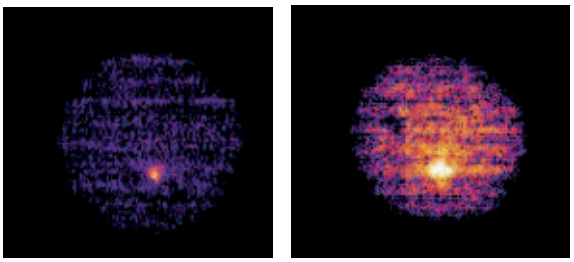

Figure 3. X-ray pin hole images (Cu K_α) for guided (250 μm long, 50 μm diameter Fe wire in Al) and reference targets (250 μm Fe foil).

Guiding of the electrons was observed by comparing foils of a given thickness with structured targets of the same thickness (eg. Reference foil thickness = wire length). Figure 3 shows a comparison between an Fe foil and structured target. The reduction in source size is clearly visible. Also visible is the significant reduction in signal outside the main spot. The FWHM of the K_α source measured on the reference foil targets is in good agreement with a recent study[17]. By contrast the size of the K_α emission region from the structured targets is of the same order as that observed for foils of <15 μm thickness. This demonstrates that the collimation effect is indeed strong and that a very large fraction of the electrons reaching the rear surface are indeed confined to the Fe wire.

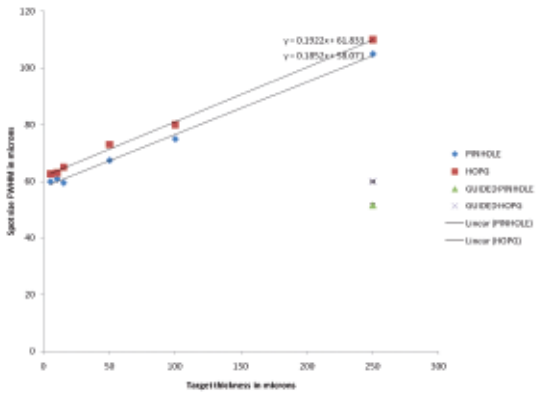

Figure 4. Graph depicting the spot size variation with thickness of target calculated from images obtained from HOPG crystal and X-ray pinhole.

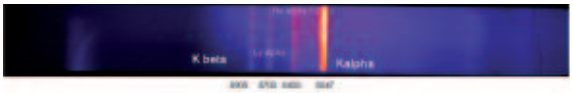

Figure 5. A typical image recorded by HOPG crystal for 15 µm Cu foil indicating the Bragg diffracted line spectra.

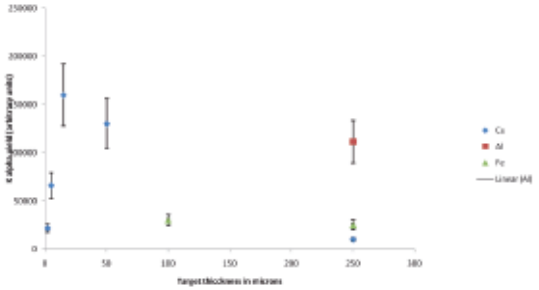

Figure 6. Integrated K_α yield calculated from HOPG spectrum for thicknesses 5-250 µm (Al and Fe targets were coated with 10 µm Cu at the rear; 2-5 µm targets are mass limited).

The efficiency of the guiding can be estimated from the integrated K_α yield. Figure 6 shows the variation of photon yield with target thickness. The result for plain foils is in good agreement with the simulations by Salzmann *et al.*[21], which predicts that for thick targets the strength of the Cu K_α emission should decay exponentially due to electron stopping in the target. Note that the electron stopping power for the 250 µm Al is comparable to 75 µm Cu are equivalent which is in agreement with their stopping powers for photons according to their mass numbers.

A direct comparison of the K_α yield obtained for 250 µm Fe reference targets and guided targets shows that to within the uncertainty of the measurement, there is a high trapping efficiency inside the wire. Given the significant shot to shot variations a lower bound for the trapping efficiency over 250 µm of about 70% can be inferred. Given that the length of the target is substantially longer than envisage for fast ignition and that the losses are likely to be higher for the highest energy electrons dominant at 250 µm length Fe targets, this is highly encouraging and likely fully adequate for fast ignition. The appearance of bright K_β line in the guided target confirms that the electrons are well collimated and produces a hot X-ray source when compared to the reference target. A significant decrease in K_α yield is observed for thin

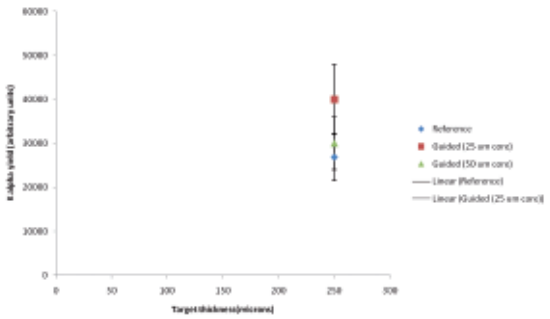

Figure 7. Integrated K_α yield calculated from HOPG spectrum for guided and reference targets.

mass limited foils which might be due to several effects like an increased volumetric heating might lead to a depletion of cold material, and an increased transfer of hot-electron energy into channels other than K_α emission for very low volume targets, notably ion acceleration might quench the inner shell signal.

Conclusion

In conclusion we have developed a technique for collimating a beam of fast electrons produced by irradiating a target with radially varying atomic number Z. The fast electrons are collimated by the self-generated azimuthal magnetic field and trapped in the high Z wire. Such targets allow substantially higher design flexibility for the fast ignitor and may have a substantial impact on ignition facility design.

References

1. D. W. Forslund, J. M. Kindel, K. Lee, *et al.*, *Phys. Rev. A* **11**, 679 (1975).
2. F. Brunel, *Phys. Rev. Lett*. **59**, 52 (1987).
3. W. L. Kruer and K. Estabrook, *Phys. Fluids* **28**, 430 (1985).
4. M. Santala *et al.*, *Phys. Rev. Lett*. **84**, 1459 (2000).
5. F. Pisani *et al.*, *Phys. Rev. E*, **62**, 5927 (2000).
6. R. B. Stephens *et al.*, *Phys. Rev. E*, **69**, 066414 (2004).
7. M. Borghesi *et al.*, *Phys. Rev. Lett*. **92**, 055003 (2004).
8. A. J. Mackinnon *et al.*, *Rev. Sci. Instrum.* **75**, 3531 (2004).
9. J. J. Santos *et al.*, *Phys. Rev. Lett*. **89**, 025001 (2002).
10. M. Tabak *et al.*, *Phys. Plasmas* **12**, 057305 (2005).
11. R. Kodama, P. A. Norreys, K. Mima, *et al.*, *Nature* **423**, 1005 (2004).
12. A. P. L. Robinson and M. Sherlock, *Phys. Plasmas* **14**, 4083105 (2007).
13. S. Kar, *et al.*, *Phys. Rev. Lett*. **102**, 055001 (2009).
14. A. W. Moore, *Highly oriented pyrolytic graphite*, *Chemistry and Physics of Carbon*, vol. 11, Marcel Dekker, New York, 1973.
15. F. J. Marshall and J. A. Oertel, *Rev. Sci. Instrum*. **68**, 735 (1997).
16. B. Dromey *et al.*, *Rev. Sci. Instrum*. **75**, 645 (2004).
17. K.Lancaster *et al.*, *PRL* **98**, 125002 (2007).
18. W. H. Zachariasen, *X-ray Diffraction in Crystals* (Wiley, New York, 1945).
19. G. E. Ice, *Nucl. Instrum. Methods Phys. Res. A* **291**, 110 (1990).
20. A. A. Hauer, N. D. Delamater and Z. M. Koenig, *Laser Part. Beams* **9**, 3 (1991).
21. D. Salzmann *et al.*, *Phys. Rev. E*, **65**, 36402 (2002).